





Observed deformation characteristics of a deep excavation for the spring area in Jinan, China

ZHANG Ding-wen¹  <http://orcid.org/0000-0003-1602-5205>; e-mail: zhangdw@seu.edu.cn

SHU Ji-cheng^{1*}  <http://orcid.org/0000-0003-3953-335X>;  e-mail: 230149191@seu.edu.cn

SUN Jian-ping²  <http://orcid.org/0000-0002-3041-6117>; e-mail: jpsun1@sina.com

* Corresponding author

¹ Institute of Geotechnical Engineering, School of Transportation, Southeast University, Nanjing 210096, China

² School of Civil Engineering, Shandong Jianzhu University, Jinan 250014, China

Citation: Zhang DW, Shu JC, Sun JP (2017) Observed deformation characteristics of a deep excavation for the spring area in Jinan, China. Journal of Mountain Science 14(3). DOI: 10.1007/s11629-016-4038-8

© Science Press and Institute of Mountain Hazards and Environment, CAS and Springer-Verlag Berlin Heidelberg 2017

Abstract: The observed deflections and internal forces of pile-anchor retaining excavation were studied in spring area in Jinan city of China. Based on field measured data, the ground surface settlement, deflection of retaining piles and wall, internal force analysis of concrete piles, axial anchoring forces, groundwater table, and the deformation of surround building and pipelines were investigated. The results indicates that the combining application of concrete piles, jet grouting columns and anchors support system can effectively control excavation-induced surface ground settlements. The field maximum lateral wall deflections are between 0.02% and 0.19% of the excavation depth due to the competitive site conditions. The bending moment-depth relationship curve is S-type. Groundwater leakage results in the sharp drop in groundwater level, which is part of the reasons for the adjacent building settlement. The axial anchoring forces of the upper layer of anchors increase gradually during the excavation, but those of the lower layer of anchors slightly reduced firstly and then tend to be stable during the excavation procedure. In comparison with the histories of excavation cases, the small lateral wall deflection in this study results from the favorable site condition and the relative rigidity of the retaining structure system.

Keywords: Spring area; Excavation; Pile anchor system; Ground settlement; Horizontal displacement

Notation

| | |
|-------------------|--------------------------------|
| w | Water content |
| γ | Unit weight of soil |
| e | Void ratio |
| I_P | Plastic index |
| I_L | Liquid index |
| k | Permeability of soil |
| E_{St-2} | Constrained modulus |
| c | Cohesion intercept |
| φ | Friction angle |
| α_{1-2} | Coefficient of compressibility |
| N | Standard penetration test |
| $N_{63.5}$ | Heavy dynamic penetration test |
| H | Excavation depth |
| δ_v | Ground settlement |
| $\delta_{h, max}$ | Maximum piles deflections |
| $\delta_{v, max}$ | Maximum ground settlement |

Introduction

Nowadays, a number of excavations have been increasing in many big cities around the world. The

Received: 12 May 2016
Revised: 27 October 2016
Accepted: 6 January 2017

underground structures, such as metro lines and underground space basements, have been constructed more and more deeply today. The monitoring of the wall deformation and ground movement is important during the excavation process (Whittle et al. 1993; Ou et al. 1998; Long 2001; Finno et al. 2002; Whittle et al. 2006; Leung and Ng 2007; Xu et al. 2008; Sun et al. 2010; Liu 2011; Tan and Li 2011; Zheng et al. 2011; Long 2012a; Whittle et al. 2015). Field monitored data and numerical stimulation of excavations have been studied by many researchers. Ou et al. (1998) documented the performance of diaphragm walls constructed using a top-down method. Ng (1998) described the performance of the multi-propped excavation in the stiff clay. Long (2001) summarized the deformation data of retaining walls and ground movements during deep excavations. Finno et al. (2002) studied the performance of a stiff supporting system in soft clay. Leung and Ng (2007) investigated the wall deformations and ground movements by cast in situ wall associated with deep excavations. Long (2012b) discussed excavation induced retaining wall deformation behavior in Dublin's estuarine deposits. Whittle et al. (2015) simulated the prediction and performance of deep excavations in Boston. In the initial excavations design, a comprehensive understanding of the characteristics of wall deformations and ground movements are great helpful. The behavior of deep excavations is dominated by many important factors, such as the type of walls, stiffness of supporting system, site condition, construction process, climate changes, and schedule. Therefore, the prediction of the wall deformation and ground movement induced from excavation is a challenging task.

Because excavation induced wall performance is a thorough reflection of various factors involved in a real excavation, analysis on the field monitored performance of previous deep excavation cases provides a useful guide for the prediction or model analysis of a new deep excavation. In the past few decades, a number of semi-empirical approaches for the excavation induced deformation have been extensively investigated by many researchers (Peck 1969; Goldberg et al. 1976; Mana and Clough 1981; Ou et al. 1993; Hsieh and Ou 1998; Long 2001; Wang and Xu 2010; Sun et al. 2012; Zheng and Li

2012; Whittle et al. 2015). These studies not only have promoted the cognitions of the performance of deep excavations, but also are useful to designers or practitioners who would check the rational numerical analysis of an excavation.

Jinan city is the capital of Shandong province, China. The design and construction of the deep excavation in Jinan depend on local experience to a large extent, so the field monitoring is important for the safety of the deep excavation. In this study, the observed deflections and internal forces of pile-anchor retaining excavation of a case are reported in details. The site conditions are presented briefly and then the observed displacements resulted from the excavation are analyzed, including ground settlement, deformation of crown beam and supporting piles, axial forces of anchor, groundwater table levels, settlement of adjacent building and utility pipelines. The lateral displacements of different types for typical supporting systems in literatures are compared. Finally some guidance is proposed for the design and construction of similar works in the future.

1 Site Conditions

Jinan city locates on the boundary of a south hilly terrain and a north plain landforms. The southern mountains are composed of limestone, which was formed about 400 million years ago. The slope of the limestone is about 30 degree from south to north. There are some fractures and caves in the limestone, which could store and transport the groundwater. Consequently, a lot of groundwater could flow into Jinan city along the slope of limestone. The texture of igneous rock below the plain is dense and impermeable, so the groundwater current is obstructed by the igneous rock. Therefore, a large number of groundwater flush into the ground through with strong pressure and the spring is born. There are more than 100 springs with different spring height in the urban area of Jinan city. For example, the water head height of Baotu Spring is 27.1 meter, and that of Five-dragon-pool Spring is 26.2 meter. The emission quantity of the Jinan's springs is 4 m³/sec and the emission quantity of Baotu Spring is about 70000 m³/day.

There are four springs in Jinan City, i.e. Baotu

Spring, Pearl Spring, Black-tiger Spring, and Five-dragon-pool Spring. The investigated excavation site is located in the west of spring core area, which is 260 m away from Five-dragon-pool Spring in the northeast, 680 m away from Baotu Spring in the southeast, 1900 m away from Black-tiger Spring in the southeast, and 1250 m away from Pearl Spring in the northeast. Figure 1 shows the positional relationship of the four springs and investigated excavation site.

During the primary geotechnical explore of excavation site, no spring was founded. However, a large amount of water poured from the underground into the excavation pit from two points when the excavation depth reached to 8 m. Then a supplementary geotechnical investigation was carried out. The emission quantity of one spring is 600 m³/day, and that of the other spring

is 700 m³. The emission of water and water pressure would damage the raft foundation. Therefore, two well point dewatering systems were installed nearby each spring in order to lower the groundwater levels. The out volume of water for well point dewatering system was about 500 m³/day. The underground water level was maintained at about 2 m below the final excavation level. The quality of the spring water is presented in Table 1.

The soil conditions were investigated using a series of soil exploration method (e.g., boreholes, wave velocity test, and standard penetration test). Figure 2 shows a typical soil profile and geotechnical parameter ranges in this excavation site. The excavation site has thick clay soils comprising quaternary artificial fill and holocene-pleistocene alluvial layer.

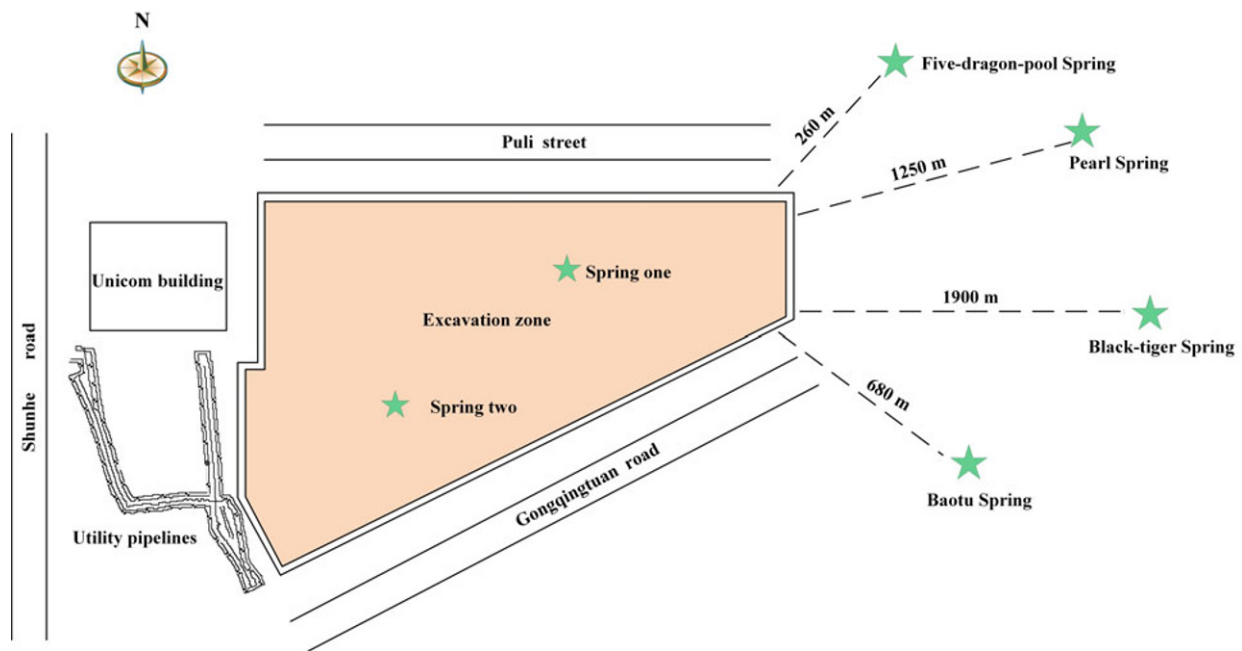


Figure 1 Location of excavation site (not to scale).

Table 1 The quality of the spring water in Jinan city (mg/L)

| Site | Month | Salinity | Ca ²⁺ | Mg ²⁺ | K ⁺ | Na ⁺ | Cl ⁻ | SQ ₄ ²⁻ | CQ ₃ ²⁻ | NQ ₃ ⁻ |
|-------------------------|---------|----------|------------------|------------------|----------------|-----------------|-----------------|-------------------------------|-------------------------------|------------------------------|
| Baotu Spring | July | 594.8 | 90.2 | 22.1 | 1.1 | 35.3 | 51.42 | 77.06 | 300 | 52.7 |
| | October | 550.2 | 87.2 | 18.5 | 0.9 | 30.2 | 45.3 | 70.2 | 289.3 | 50 |
| Pearl Spring | July | 703.9 | 86.9 | 21.4 | 1.5 | 65 | 94.1 | 125.9 | 257.5 | 43.5 |
| | October | 468.4 | 82.2 | 16.1 | 0.8 | 35.7 | 50.4 | 92.8 | 237.7 | 25.5 |
| Black tiger Spring | July | 646.1 | 122.2 | 23.1 | 0.5 | 18.6 | 54.9 | 87.3 | 296.9 | 40.2 |
| | October | 586.3 | 106.1 | 20.4 | 0.4 | 14.3 | 39.6 | 80.5 | 274.1 | 39.6 |
| Five-dragon-pool Spring | July | 753.3 | 142.1 | 32.9 | 0.7 | 25.7 | 82.8 | 121.5 | 325.8 | 83.2 |
| | October | 723.5 | 140.5 | 27.8 | 0.5 | 22.8 | 71.6 | 99.6 | 290.9 | 79.2 |
| This study | July | 582.3 | 85.6 | 20.1 | 1.2 | 32.2 | 50.3 | 70.1 | 285 | 51.2 |
| | October | 576.2 | 75.2 | 17.3 | 0.8 | 28.3 | 50.1 | 53.2 | 270.2 | 43.2 |

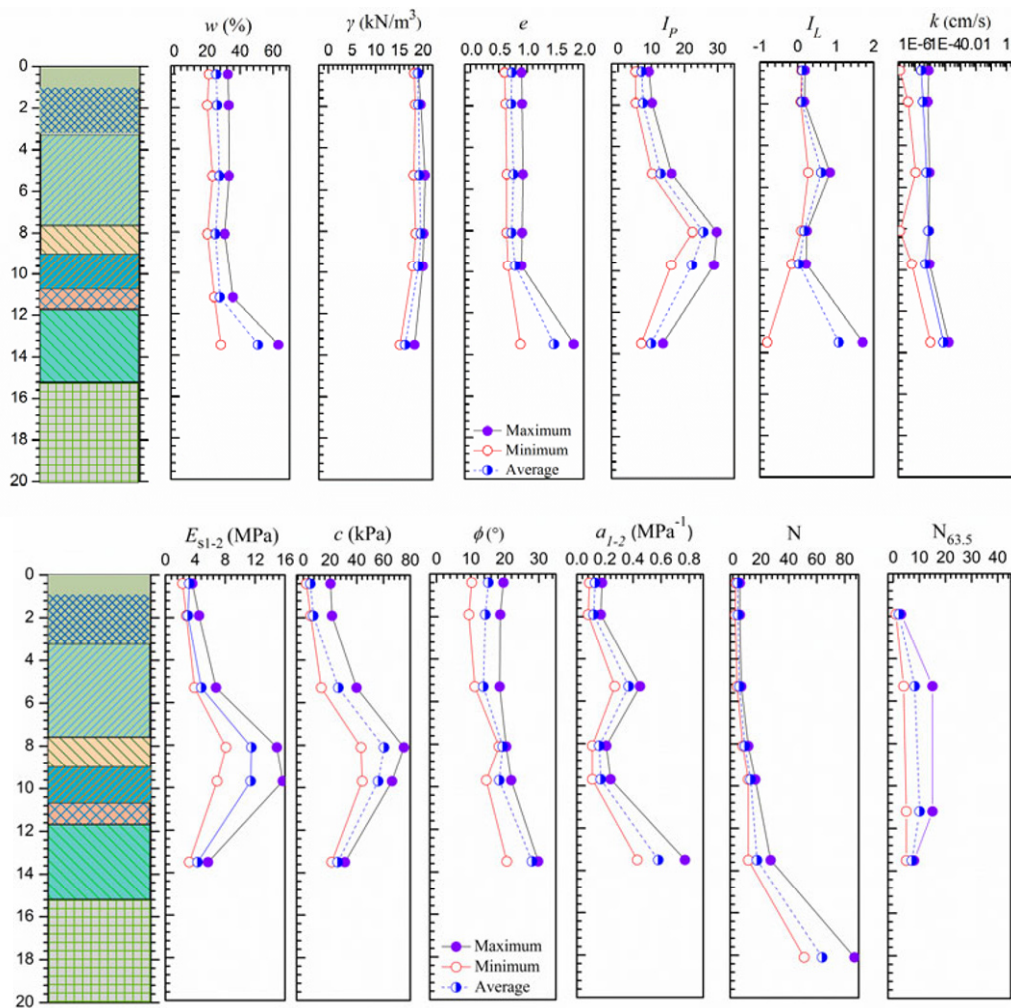


Figure 2 Soil profiles and geotechnical parameters.

The top upper layer was formed by artificial fill with a thickness of 2.2 to 3.1 m. Underlying is silty clay with medium plasticity and the average thickness of this layer is 4.4 m. The third layer is tawny clay with a thickness of 0.8 to 3.5 m which is medium plasticity and high toughness. Below this stratum is brown stiff clay with a thickness of 0.4 to 6.8 m which is deposited in the medium Pleistocene geological period. Beneath this layer is a gravel layer with a thickness of 0.8 to 7.9 m. It is poor uniformity. The sixth layer is a sandy soil with a thickness of 1.3 to 10 m which comes from diorite rock. The next layer soil is strongly weathered diorite with a thickness of 0.6 to 9 m. The last layer is medium weathered diorite. The diorite core is very brittle with rock core recovery of 60% to 80% and Rock Quality Designation (RQD) of 50% to 70%.

The groundwater table is generally 1.9 to 5.0 m

below the ground surface. The coefficients of permeability of silt clay, tawny clay, and stiff clay are $5.72E^{-06}$ cm/sec, $7.50E^{-06}$ cm/sec, and $4.86E^{-06}$ cm/sec, respectively. The cohesion of the second layer ranges from 13.4 to 39.8 kPa. The standard penetration test blows (N) of this layer ranges from 3 to 6. The cohesion of the third layer ranges from 43.2 to 75.2 kPa and the average N is 8.5. The cohesion of the fourth layer ranges from 44.1 to 66.3 kPa and the average N is 12.6.

2 Project Information and Construction Procedure

2.1 Project information

The investigated excavation is for the basement of a 300 m high skyscraper. The

excavation is close to the Pulistreet on the north side, and the horizontal distance from the excavation boundary to the Puli street ranges from 24.3 to 25.3 m. The Gongqingtuan road is on the southeast side of the excavation. The horizontal distance from the excavation boundary to the Gongqingtuan road ranges from 16.6 to 21.4 m. An existed building named Unicom building is on the west side of the excavation site, and the external wall of the basement are from 5.0 m away from the Unicom building. The main pipelines are four utility pipelines with a diameter of 1500 mm on the west of investigated excavation site. The burial depth of the pipelines varies from 0.8 to 1.8 m below ground surface. The minimum horizontal distance between the utility pipelines and excavation boundary is 3.0 m.

2.2 Construction sequence

Figure 3 shows the support systems of the typical section of excavation. The support system is divided into AB, BC, CD and DA four sections. Concrete piles, jet grouting columns and anchors were designed to support the excavation.

The cast-in site concrete piles were rock-socketed piles to provide lateral stability and effective cutoff of groundwater. The diameter of concrete piles was 800 mm and the embedded depths of concrete piles below pit were 8 m to 15 m. The spacing of cast-in site concrete piles was 1800 mm. Due to the high groundwater table; jet grouting columns were constructed for sealing, which were 20 m in length and 800 mm in diameter. Two layers of anchors with a vertical spacing of 4.5 m were used for the support system. The length of upper anchors ranged 23.5 m to 26 m and that of lower anchors were 16 m to 18.5 m. The angle between the axis of anchor and the horizontal plane was 15 degree. Preloads range from 38 kN to 195 kN were exerted onto the anchors in order to reduce the displacement of support system and the ground settlement. The design parameters of anchors used in this case are shown in Table 2.

Figure 4 briefly illustrates the construction procedure at the site. The excavation construction was divided into eight steps. It started with the construction of cast-in site concrete piles. After the installation of cast-in site concrete piles, the jet grouting columns for sealing were constructed.

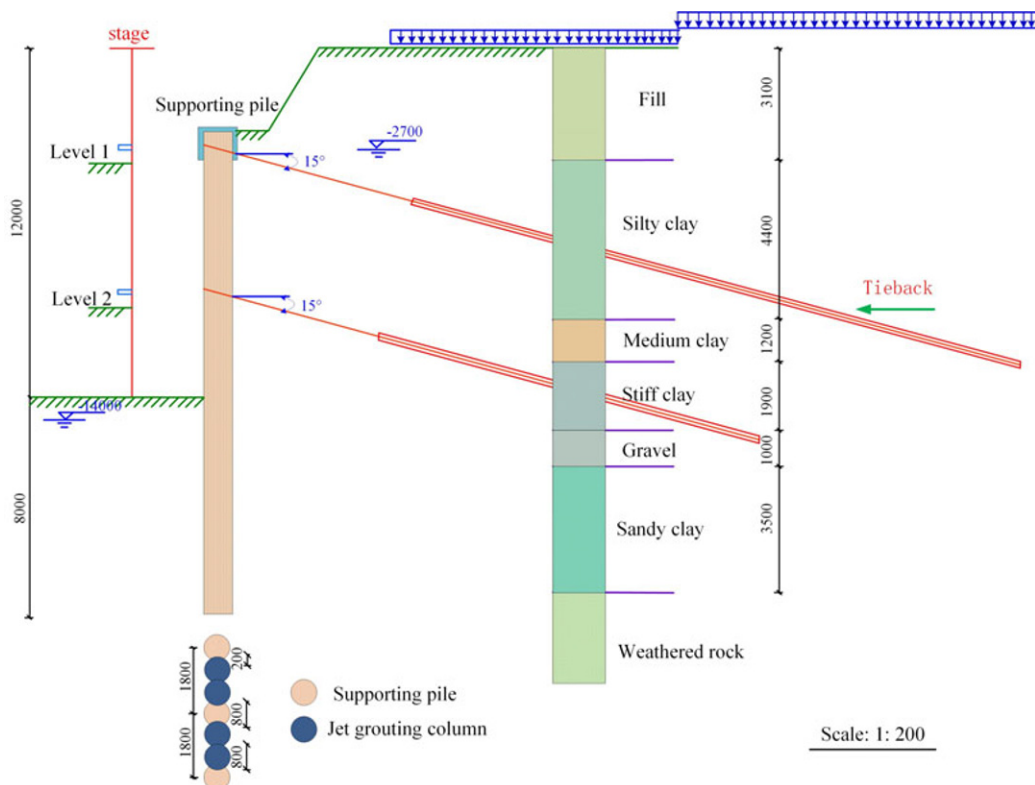


Figure 3 Support systems of typical section.

Before the first layer excavation with depth of 4.2 m, the groundwater table was dewatered to 6.2 m from the surface. After finish the first layer excavation, the upper layer anchors were installed with a high grouting pressure (2 MPa to 3 MPa). Then, the groundwater table was continually dewatered to 10.2 m and the pit was excavated to 8.2 m from the ground surface. The lower layer anchors were installed with a high grouting pressure (2 MPa to 3 MPa). At last, the groundwater table was continually dewatered to 14 m and the pit was excavated to 12 m. Once the excavation was completed, the raft foundation was constructed.

2.3 Monitoring instruments

To confirm design scheme and monitor the performance of excavation for securing the safety of this project, various instruments were installed in situ. Figure 5 shows the site instrumentation layout of this study.

Ten ground surface settlements gauges (designated as D1 to D10) were installed perpendicularly to the Pulistreet and Gongqingtuan Road. A borehole was drilled and a steel section with a length of 150 mm and a diameter of 20 mm was hammered into the bore hole. The excess hole was filled with cement mortar and then a ground surface settlement gauge was

Table 2 Design parameters of anchors used in this case.

| Location | | Anchor length (m) | Horizontal spacing (m) | Preload (kN) |
|----------|-------|-------------------|------------------------|--------------|
| AB | Upper | 26 | 2.7 | 50.2 |
| | Lower | 16 | 2.7 | 38.2 |
| BC | Upper | 25 | 1.8 | 180.2 |
| | Lower | 18 | 1.8 | 90.2 |
| CD | Upper | 23.5 | 2.7 | 72.3 |
| | Lower | 16 | 2.7 | 153.6 |
| DA | Upper | 25.5 | 1.8 | 195.6 |
| | Lower | 18.5 | 1.8 | 85.2 |

Note: AB, BC, CD and DA are four sections of the support system.

formed. These settlement points were arranged with a space of 5 m, so the settlements gauges D1 to D5 distanced from 5m to 30 m away from the concrete piles.

The horizontal deflections of concrete piles were measured using three inclinometer tubes (designated as L1 to L3, as shown in Figure 5). Figure 6(a) presents the pictures of inclinometer tubes in concrete piles. Twelves train gauges are also used to measure the strain of concrete piles during the excavation. Figure 6(b) shows the pictures of strain gauges welded on steel reinforcement cage of concrete piles. Twenty six wall deflection gauges (designated as Q1 to Q26, as shown in Figure 5) were installed to monitor the horizontal displacements of the top of wall. The groundwater tables outside excavation pit were monitored by ten groundwater level pipes

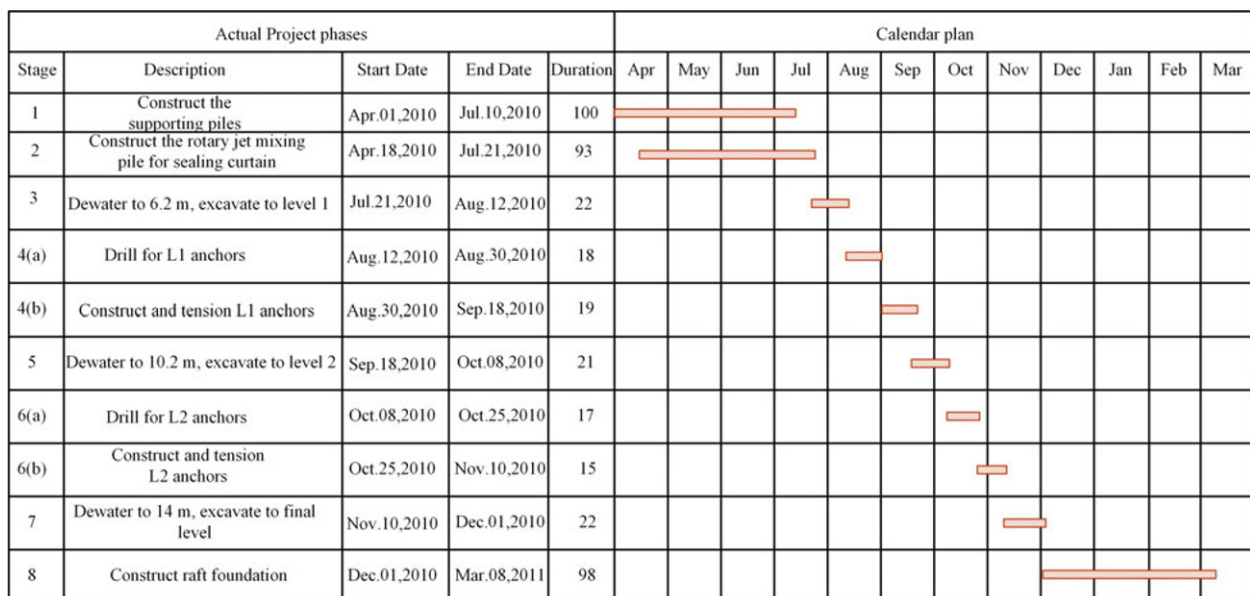


Figure 4 Schedule of construction procedure.

(designated as W1 to W10), which were buried to a depth of 17 m from the ground. In order to measure the development of axial force of anchors, six vibrating wire strain gauges for anchors (designated as A1 to A6) were used. Figure 6(c) shows the pictures of anchor strain gauge. A1, A3 and A5 are assigned to the upper layer of anchors and A2, A4 and A6 are assigned to the lower layer of anchors.

Unicom building was adjacent to the excavation boundary 7 m away and utility pipelines were adjacent to the excavation boundary 3 m away. In order to insure the safety of the surrounding building and utility pipelines during the excavation, twelve deflection points (designated as J1 to J12) and four deformation points (designated as P1 to P2) were installed on the walls of Unicom building and on the top of utility pipelines, respectively.

All the field monitor items of the deflections about the excavation, Unicom building, utility pipelines were recorded twice a day from during the stage 3 to stage 7, and one time every day during construction of the raft foundation (i.e. stage 8). The field readings of internal force of piles and anchors were recorded one time every day

from stage 3 to stage 7, and one time every two days during construction of the raft foundation (i.e. stage 8). The groundwater table levels were measured twice a day throughout the excavation and construction period.

3 Test Results

3.1 Horizontal deflections of concrete piles

Lateral deflections of concrete piles were obtained from three inclinometers. Figure 7 presents the horizontal deflections of concrete piles measured at L1 of the north segment, L2 of the south segment, and L3 of the west segment. The results show that the deformations of the concrete piles increase with the increase of excavation depth, and it come to the maximum when the construction of the raft foundation is finished. With the tension of anchors, there is a slight rebound for horizontal deformation of concrete piles. Therefore, the anchors play a significant role in reducing the horizontal displacement of concrete piles induced from excavation. The horizontal

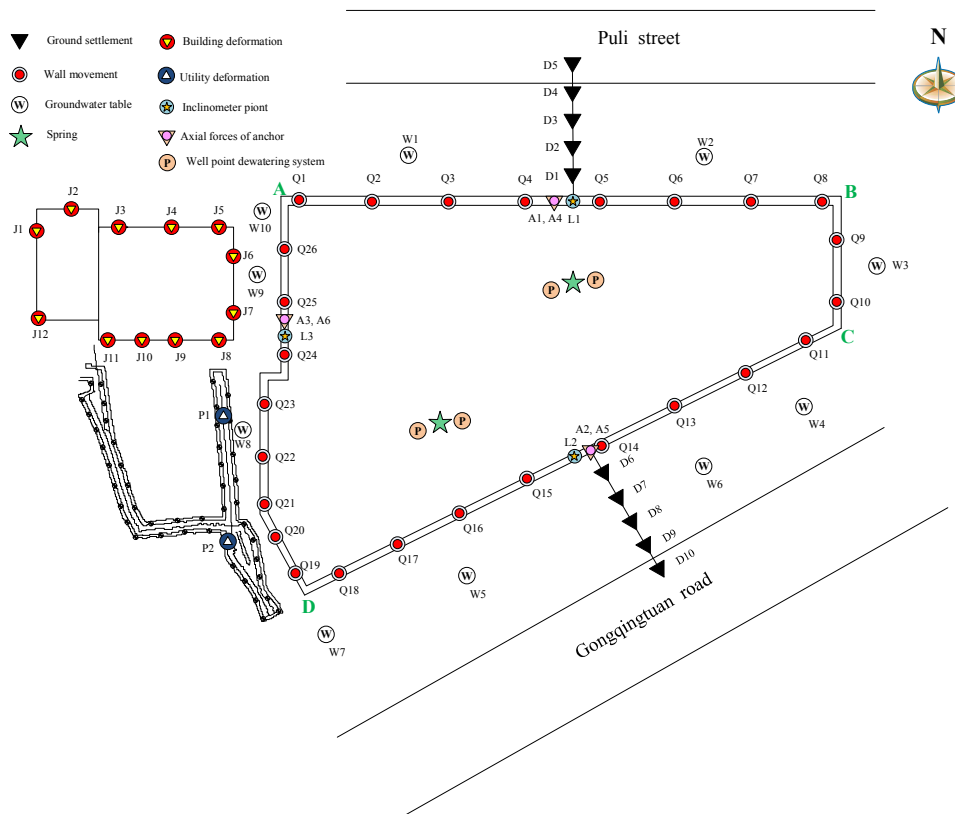


Figure 5 Layout of instrumentation gauges.

deformations of concrete piles are less than 1 mm after the first row cables tensioned at the beginning of excavation. With the continued excavation construction, the displacements increase gradually to 7mm after the excavation depth reach to 8.2 m. The displacements increase gradually to 9 mm until the excavation depth come to 12 m, which is 0.08 percent of the excavation depth. Figure 7 also shows that the horizontal displacements concrete piles decrease with the increasing depth.

3.2 Internal force analysis of concrete piles

Figure 8 presents the bending moment of concrete piles with the depth during the excavation. The bending moments of supporting piles increase gradually and the position of maximum value shifts downward with the increasing of excavation depth. Figure 8 shows the position of maximum positive moment corresponds to the position of the maximum horizontal displacement. It is shown that the relationship between bending moment of concrete piles with the depth gradually becomes an S-type curve after the excavation depth reach to the final level (i.e. 12.0m). The negative bending moment is in line with inflection point of piles displacement in final level.

The original moment distribution changes when the anchors are applied to supporting piles. For example, Figure 8 shows that the maximum bending moment of supporting piles is 40kN·m prior to the first row anchors tensioned and bending moment reduces to 35 kN·m after the anchors tensioned at the north side of excavation. Prior to the second row anchors construction, the maximum bending moment is 55 kN·m and the bending moment fall to 50 kN·m after the second row anchors tensioned. The bending moment records 98 kN·m after the excavation depth reach to the final level (i.e. 12.0 m) and it changes negligibly after the raft foundation was construction. The relationship curves of bending moment and depth of the south shaft and the west shaft are similar to that of the north shaft, which indicates that anchors tension has a great influence on the bending moment of supporting piles.

3.3 Ground surface settlement

Figure 9 shows the ground settlement



Figure 6 Field monitoring instruments. (a) inclinometer; (b) strain gauge; (c) anchor strain gauge.

measurement results. In this study, the ground settlement (δ_v) is less than 10 mm. Comparing with these reported in Singapore stiff clay (i.e., 0.1%) and in Taiwan soft clay (i.e., 0.2%), the measured δ_v/H ratio (settlement normalized by excavation depth H) is less than 0.072% and is smaller in this study.

Peck (1969) proposed an empirical approach to predict excavation-induced ground settlement based on field observations. He established the relation curves between the normalized ground settlement (δ_v/H) and the normalized distance from the wall (d/H) for different types of soil, as shown in Figure 9. The relationship classified into Zone I, Zone II, and Zone III according to the type of soil. Most field data of this excavation case falls within Zone I and is far away from Zone III. This means that the combining application of concrete piles, jet grouting columns and anchors support system can effectively control excavation-induced surface ground settlements in this type of site condition.

3.4 Horizontal displacement of top of wall

Figure 10 shows the horizontal displacement of top of AB and CD segments wall during excavation. As shown in Figure 10, the horizontal displacement curves have a stepped upward trend. By April, 2011, the maximum horizontal displacement of AB segment wall reached 9 mm, and that of CD segment wall reached 7 mm. The monitoring points located in the middle of wall show the maximum horizontal displacement. The horizontal displacement of Q5 is larger than other points located on the AB segment and that of Q14 is larger than other points of CD segment.

3.5 Maximum lateral wall deflection

Figure 11 shows the relationship between the maximum lateral wall deflection ($\delta_{h,max}$) and excavation depth. To compare the deformation performance of different excavation cases, many published case histories of excavations in soft to medium clays are collected. Table 3 shows the information on the soil properties and supporting form of excavations cases.

The results indicate that the maximum lateral wall deflections in this project are between 0.02% and 0.19% of the excavation depth. By comparing excavations case histories, it is observed that the maximum lateral wall deflection in this study is similar with that in Dublin-Jervis due to the similar favorable soil conditions. In addition, it is observed that most of the measured $\delta_{h,max}$ values in Singapore and San Francisco are between 0.38% and 1.6% of the excavation depth, which are above the range of 0.19% and 0.56% of the excavation depth measured in Shanghai, Taipei, and Boston. The excavations in Singapore, San Francisco, Shanghai,

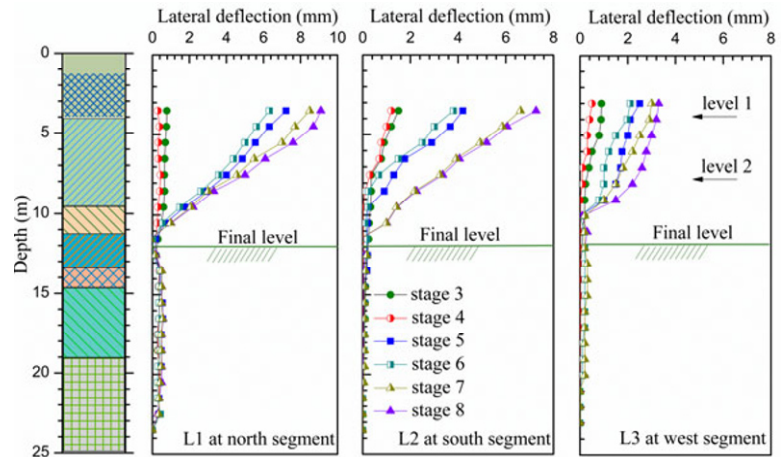


Figure 7 Horizontal deformations of concrete piles.

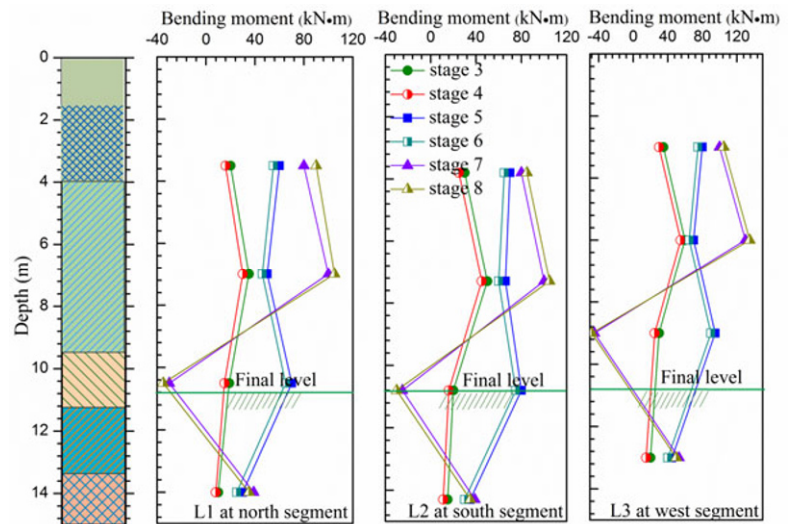


Figure 8 Bending moment of concrete piles.

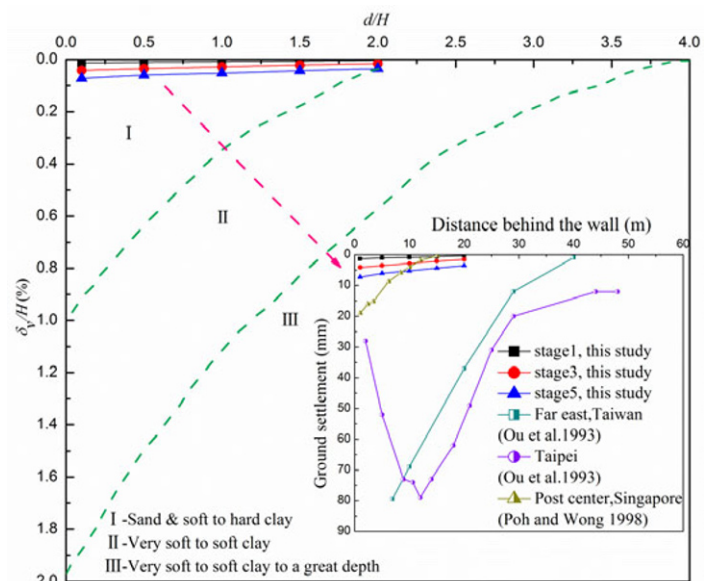


Figure 9 Normalized settlement profiles adjacent to excavations.

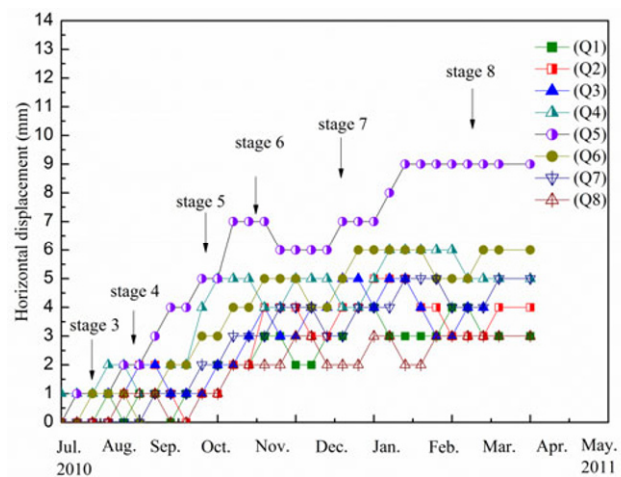
Taipei, and Boston are all constructed in soft soils. This outcome is also attributed to the fact that the excavations in Shanghai, Taipei and Boston are usually supported by diaphragm walls, while the excavations in Singapore and San Francisco are supported by contiguous bored pile walls and sheet piles.

3.6 Relationship between the maximum ground settlement and the maximum piles deflection

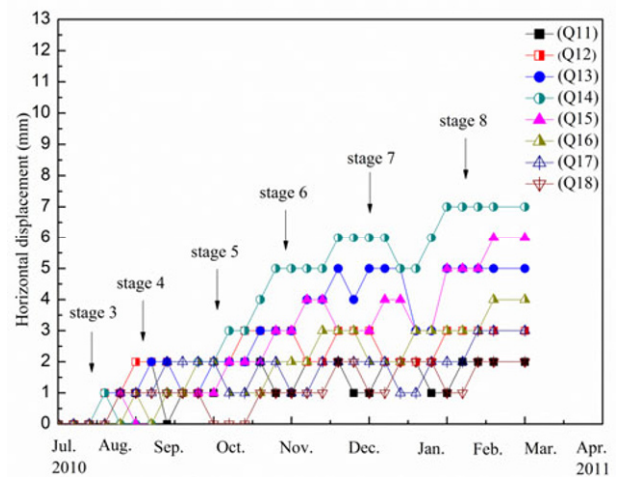
Figure 12 presents the relationship between the maximum ground settlement ($\delta_{v,max}$) and the maximum piles deflections ($\delta_{h,max}$). Mana and Clough (1981) summed up the relationship between the normalized maximum ground settlement and the maximum wall movement using the data from many excavation cases in San Francisco, Oslo, and Chicago. According to Mana and Clough (1981), most of the excavations show that the maximum ground settlement ranges from 0.5 to 1.0 time the maximum piles deflections. Wallace (1993) and Ou (1993) also sorted out field data from excavations in Singapore and Taipei, respectively. Wallace (1993) reported that the maximum ground settlement almost equal to the maximum piles deflections for excavation in Singapore city. Ou (1993) reported that the maximum ground settlement almost equal to 0.6 time the maximum piles deflections for excavation in Taipei city. The field data from Jinan city is compared with these data in Figure 12. For this excavation, field data fall on the line $\delta_{v,max} = \delta_{h,max}$, and the trend is similar with that in San Francisco. Therefore, surrounding ground settlement could be controlled simultaneously along with controlling the displacement of supporting piles.

3.7 Groundwater table

Figure 13 shows the measured groundwater table variation outside the excavation pit with time. Before the construction stage 4 (as shown in Figure 4), the groundwater table variation is gentle. During the construction stage 5 (i.e. dewatering to 10.2 m and excavation depth reaching to 8.2 m), measured groundwater



(a)



(b)

Figure 10 Horizontal displacement of top of wall during excavation: (a) AB segment, (b) CD segment.

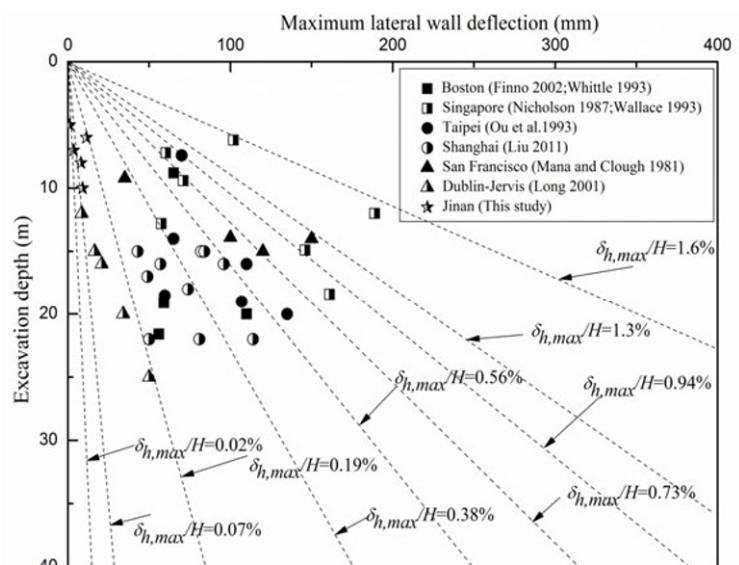


Figure 11 Maximum lateral wall deflections versus excavation depth.

table at points W1, W2, W3, W4 and W9 drop sharply and the maximum variation speed reach to was 2 m/d. This is because that a large amount of groundwater leaks from the first layer of anchor holes. After the plugging treatment of anchor holes, the groundwater tables become stable. For example, the natural groundwater table of point W9 is 4.2 m, and it drops to 9.6 m during the after excavation, which results in a 5.4 m drop of groundwater table. Due to Point W9 adjacent to Unicom building, groundwater leakage is part of the reasons for Unicom building settlement.

3.8 Axial anchoring forces

Six axial force gauges of anchor measured results during excavation are presented in Figure

14. A1, A3 and A5 are assigned to the upper layer of anchors and A2, A4 and A6 are assigned to the lower layer of anchors. As shown in Figure 14, the axial anchoring forces of the upper layer of anchors increase gradually during the excavation. The axial anchoring forces of A1, A3 and A5 increase gradually to 103.2 kN, 218.3 kN and 130.5 kN, respectively. On the other hand, the axial anchoring forces of the lower layer of anchors (A2, A4 and A6) are slightly reduced firstly and then tend to be stable during the excavation procedure.

3.9 Settlements of adjacent building

Figure 15 presents settlement monitoring results of the adjacent unicom building. The positive value indicates an upward displacement

Table 3 Comparison of wall deflections of cases

| Sources | Location | Ground conditions | Support type | $\delta_{h, max}/H(\%)$ |
|------------------------|---------------|---------------------------|--|-------------------------|
| Goldberg (1976) | Worldwide | Silty clay | Sheet piles | <0.35 |
| Mana and Clough (1981) | San Francisco | Soft clay | Sheet piles | 0.6~2.2 |
| Ou et al. (1993) | Taipei | Silty sand and Silty clay | Diaphragm wall and sheet piles | 0.2~0.94 |
| Masuda (1993) | Tokyo | Sand and clay | Diaphragm wall | 0.05~0.5 |
| Wallace et al. (1993) | Singapore | Stiff clay | Contiguous piles | 0.38~1.6 |
| Whittle et al. (1993) | Boston | Blue clay | Diaphragm wall | 0.12~0.73 |
| Wong et al. (1997) | Singapore | Stiff clay | Contiguous bored pile and diaphragm wall | 0.03~0.2 |
| Long (2001) | Dublin-Jervis | Glacial till | Soldier piles and sheet piles | 0.07~0.2 |
| Wang (2005) | Shanghai | Soft soil | Diaphragm wall | <0.7 |
| Kung et al. (2007) | Taipei | Clay | Diaphragm wall | 0.1~0.52 |
| Liu (2011) | Shanghai | Soft soil | Diaphragm wall | 0.2~0.56 |
| This study | Jinan | Jinan clay | Concrete piles, jet grouting columns and anchors | 0.02~0.19 |

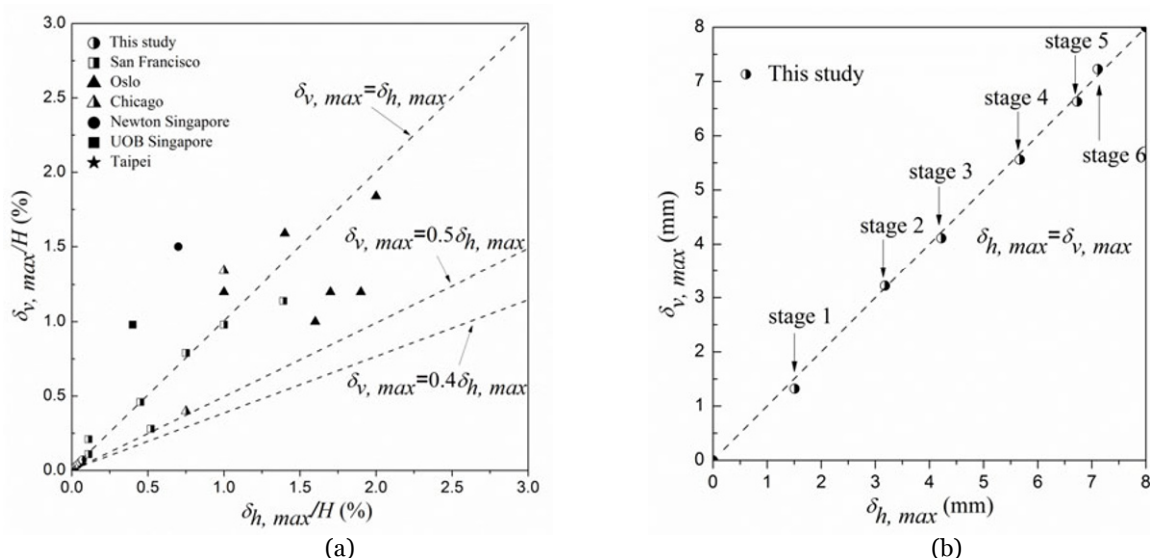


Figure 12 Relationship between the maximum ground settlement and the maximum piles deflection: (a) Combined cases date; (b) This study.

and the negative value means a downward displacement. From Figure 15, it is observed that the settlements of the unicom building go through three stages, which are a uniform subsidence stage, an accelerated subsidence stage and a stable subsidence stage. The settlements of the adjacent Unicom building increase suddenly when the excavation depth increases from 8.2 m to 12.0m. Then the settlements become stable when the basement of raft foundation begins to construction.

Point J7 locates at the southeastern corner of building and point J1 locates at the northwestern corner of building. Point J7 is adjacent to the excavation boundary 7 m away, which records the maximum value of settlement and the final settlement is 3.8mm. The horizontal distance between Point J1 and excavation boundary is 76 m, so the final settlement of point J1 is 1.0mm. The ground further away from excavation is disturbed lightly than that near the excavation. The variation of groundwater level near point J7 drops 5.4 m (as shown in Figure 13). The decline of groundwater level is the main cause of land subsidence.

3.10 Deformation of surrounding utility pipelines

There are four utility pipelines on the west of excavation with a diameter of 1500 mm and buried depth of 0.8 m to 1.8 m below ground surface. The utility pipelines are metallic materials which are surrounded by reinforced concrete.

Figure 16(a) shows the horizontal displacements of pipelines during excavation. The horizontal displacements of pipelines increase during each excavation step and decrease after the installation of anchors. The displacement curves of P1, P2 change in a similar trend. As shown in Figure 16(a), the horizontal displacement of P1 point increase firstly and decreases slightly after the upper layer of anchors being tensioned. The horizontal deformation increases from 3 mm to 6 mm before the lower layer of anchors are constructed. The horizontal displacements of P1 point decrease slightly to 4 mm after lower layer of anchors are tensioned. After that horizontal deformations increase to 6

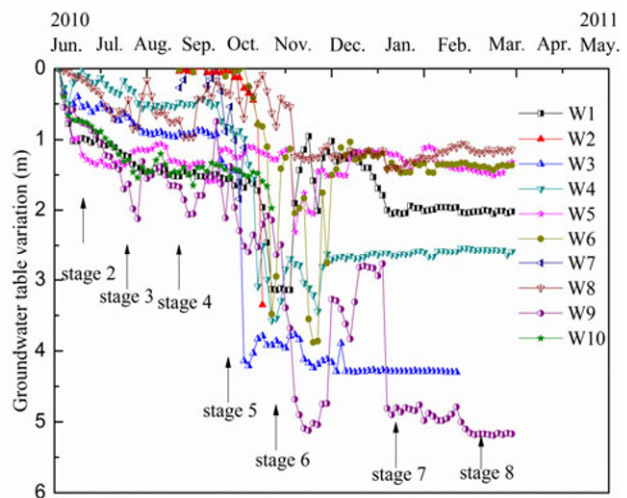


Figure 13 Groundwater table variation.

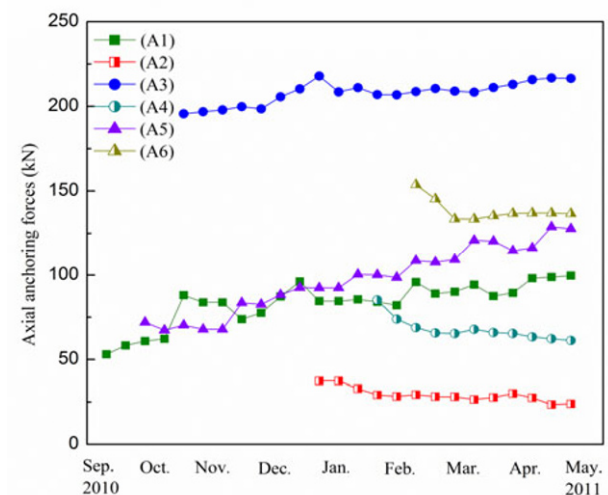


Figure 14 Axial anchoring forces during excavation.

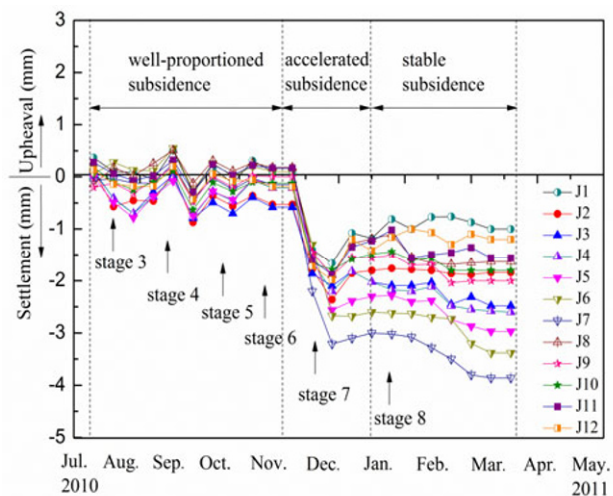


Figure 15 Settlement developments of adjacent Unicom building.

mm gradually.

Figure 16(b) shows the settlement of pipelines during excavation. The settlements increases slightly firstly and reaches to 2.5 mm after 28 days excavation. The tension of anchors results in a decrease of settlement to 0.5 mm. Settlements of pipeline rebound and become stable eventually.

3.11 Cost analysis

The diaphragm wall has relatively high stiffness and effective water tightness performance, but its cost is quite high. On the other hand, the diaphragm walls are usually adopted as the retaining wall as well as the outside wall of a basement, which can save 25 percent to 35 percent of the underground structure cost. The concrete piles are usually adopted as a temporary wall with the advantages of lower cost and higher construction speed comparing to the diaphragm wall. Combining cost analysis and supporting structure features, it could be concluded that the diaphragm walls are moresuitableforin a softsoil or coastal are as and the concrete piles are more applicable in the stiff clay.

4 Conclusions

Based on the measurements of a ground surface settlement, deflection of wall, axial anchoring forces, and the deformation of surround building and pipelines, the deformation

characteristics of a pile-anchor retaining excavation case study is presented. The following conclusions may be drawn:

(1) The measured ground surface settlement is less than 10 mm, which is classified in Zone I defined by Peck (1969). The bending moment-depth relationship curve is S-type. It indicates that the combining application of concrete piles, jet grouting columns and anchors support system can effectively control excavation-induced surface ground settlements in this type of site condition.

(2) The field maximum lateral wall deflections are between 0.02% and 0.19% of the excavation depth. The maximum ground settlement equals to the maximum wall movement. Comparing with excavation case histories, the small lateral wall deflection in this case study results from the favorable site conditions and the relative rigidity of the retaining structure system.

(3) The points in the middle of segment show a larger horizontal displacement of the top of wall than those of at two edges, and the settlements of the top of wall undergo a serrated deformation patterns.

(4) The axial anchoring forces of the upper layer of anchors increase gradually during the excavation. On the other hand, the axial anchoring forces of the lower layer of anchors are slightly reduced firstly and then tend to be stable during the excavation procedure.

(5) Groundwater leakage results in the drop sharply of groundwater table, which is part of the reasons for Unicom building settlement.

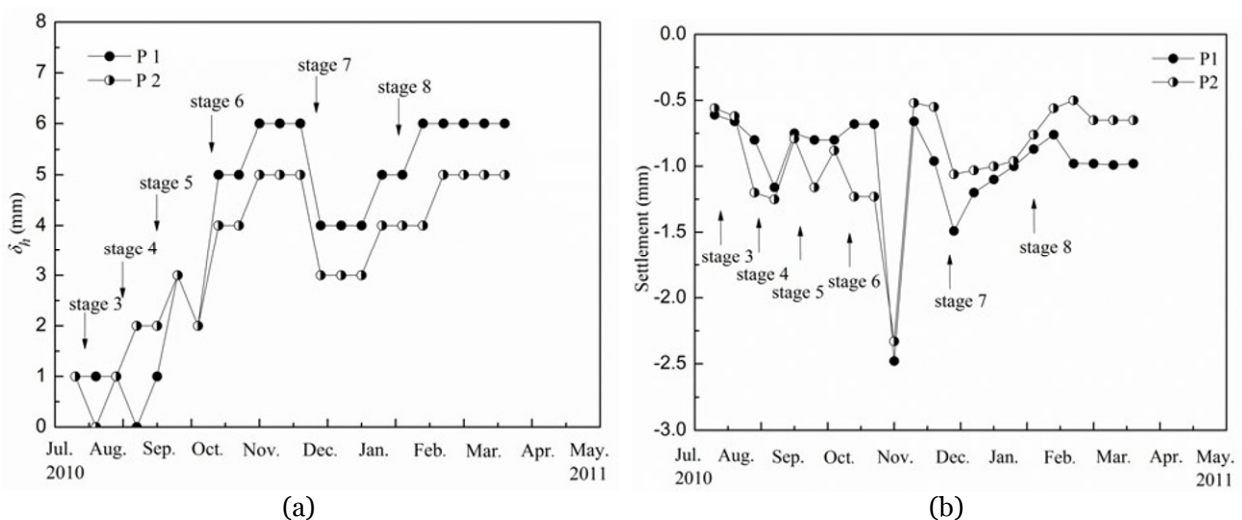


Figure 16 Deformations of utility pipelines. (a) horizontal displacement; (b) settlement.

Acknowledgements

This work was supported by the Chinese Fundamental Research Funds for the Central Universities (Grant No. 2242014R30020), and the

Personnel Training Fund for Outstanding Young Teacher of Qinglan Project of Higher Education in Jiangsu Province, China. Concrete suggestions from the reviewers, the Editors are gratefully acknowledged.

References

- Finno RJ, Bryson LS (2002) Response of building adjacent to stiff excavation support system in soft clay. *Journal of performance of constructed facilities* 16: 10-20. DOI: [10.1061/\(ASCE\)0887-3828\(2002\)16:1\(10\)](https://doi.org/10.1061/(ASCE)0887-3828(2002)16:1(10))
- Goldberg DT, Jaworski WE, Gordon MD (1976) Lateral support systems and underpinning: construction methods. Federal Highway Administration, Offices of Research & Development, Washington, D.C.
- Hsieh PG, Ou CY (1998) Shape of ground surface settlement profiles caused by excavation. *Canadian Geotechnical Journal* 35: 1004-1017. DOI: [10.1139/cgj-35-6-1004](https://doi.org/10.1139/cgj-35-6-1004)
- Kung TC, Juang H, Hsiao CL, et al. (2007) Simplified model for wall deflection and ground-surface settlement caused by braced excavation in clays. *Journal of Geotechnical and Geoenvironmental Engineering* 133:731-747. DOI: [10.1061/\(ASCE\)1090-0241\(2007\)133:6\(731\)](https://doi.org/10.1061/(ASCE)1090-0241(2007)133:6(731))
- Leung EHY, Ng CWW (2007) Wall and ground movements associated with deep excavations supported by cast in situ wall in mixed ground conditions. *Journal of Geotechnical and Geoenvironmental Engineering* 133: 129-143. DOI: [10.1061/\(ASCE\)1090-0241\(2007\)133:2\(129\)](https://doi.org/10.1061/(ASCE)1090-0241(2007)133:2(129))
- Liu GB, Jiang RJ, Ng CWW, et al. (2011) Deformation characteristics of a 38 m deep excavation in soft clay. *Canadian Geotechnical Journal* 48: 1817-1828. DOI: [10.1139/T11-075](https://doi.org/10.1139/T11-075)
- Long M (2001) Database for retaining wall and ground movements due to deep excavation. *Journal of Geotechnical and Geoenvironmental Engineering* 127: 203-224. DOI: [10.1061/\(ASCE\)1090-0241\(2001\)127:3\(203\)](https://doi.org/10.1061/(ASCE)1090-0241(2001)127:3(203))
- Long M, Brangan C, Menkiti C, et al. (2012a) Retaining wall behaviour in Dublin's fluvio-glacial deposits, Ireland. *Proceedings of the Institution of Civil Engineers-Geotechnical Engineering* 165: 351-365. DOI: [10.1680/geng.10.00037](https://doi.org/10.1680/geng.10.00037)
- Long M, Daynes PJ, Donohue S, et al. (2012b) Retaining wall behaviour in Dublin's fluvio-glacial gravel, Ireland. *Proceedings of the Institution of Civil Engineers-Geotechnical Engineering* 165: 289-307. DOI: [10.1680/geng.9.00099](https://doi.org/10.1680/geng.9.00099)
- Mana AI, Clough GW (1981) Prediction of movements for braced cuts in clay. *Journal of Geotechnical and Geoenvironmental Engineering* 107(6): 759-777.
- Masuda T (1993) Behavior of deep excavation with diaphragm wall. MSc thesis, Massachusetts Institute of Technology (MIT), Cambridge, Mass.
- Ng CWW (1998) Observed performance of multipropped excavation in stiff clay. *Journal of Geotechnical and Geoenvironmental Engineering* 124: 889-905. DOI: [10.1061/\(ASCE\)1090-0241\(1998\)124:9\(889\)](https://doi.org/10.1061/(ASCE)1090-0241(1998)124:9(889))
- Ou CY, Hsieh PG, Chiou DC (1993) Characteristics of ground surface settlement during excavation. *Canadian Geotechnical Journal* 30: 758-767.
- Ou CY, Liao JT, Lin HD (1998) Performance of diaphragm wall constructed using top-down method. *Journal of Geotechnical and Geoenvironmental Engineering* 124: 798-808. DOI: [10.1061/\(ASCE\)1090-0241\(1998\)124:9\(798\)](https://doi.org/10.1061/(ASCE)1090-0241(1998)124:9(798))
- Peck RB (1969) Deep excavation and tunneling in soft ground. State-of-the-art-report. Proc., 7th Int. Conf. of Soil Mechanics and Foundation Engineering, International Society of Soil Mechanics and Geotechnical Engineering (ISSMGE), Mexico City. pp 225-281.
- Sun JP, Shao GB, Jiang ZB (2012) Design and construction technology of displacement control in deep miscellaneous fill foundation pits. *Chinese Journal of Geotechnical Engineering*, 34(S0): 576-580. (In Chinese)
- Sun JP, Wei HW, Jiang ZB, et al. (2010) Factors for displacement of composite soil nailing walls. *Chinese Journal of Geotechnical Engineering* 32(S1): 431-434. (In Chinese)
- Tan Y, Li MW (2011) Measured performance of a 26 m deep top-down in excavation in downtown Shanghai. *Canadian Geotechnical Journal* 48: 704-719. DOI: [10.1139/t10-100](https://doi.org/10.1139/t10-100)
- Wallace JC, Ho CE, Long MM (1993) Retaining wall behaviour for a deep basement in Singapore marine clay. In *Proceedings of the International Conference on Retaining Structures*, Cambridge, UK, 20-23 July 1992. Thomas Telford, London. pp 195-204.
- Wang JH, Xu ZH, Wang WD (2010) Wall and ground movements due to deep excavations in Shanghai soft soils. *Journal of Geotechnical and Geoenvironmental Engineering* 136: 985-994. DOI: [10.1061/\(ASCE\)GT.1943-5606.0000299](https://doi.org/10.1061/(ASCE)GT.1943-5606.0000299)
- Wang ZW, Ng CWW, Liu GB (2005) Characteristics of wall deflections and ground surface settlements in Shanghai. *Canadian Geotechnical Journal* 42: 1243-1254. DOI: [10.1139/T05-056](https://doi.org/10.1139/T05-056)
- Whittle AJ, Corral G, Jen LC, et al. (2015) Prediction and performance of deep excavations for courthouse station, Boston. *Journal of Geotechnical and Geoenvironmental Engineering* 141: 1246-1259. DOI: [10.1061/\(ASCE\)GT.1943-5606.0001246](https://doi.org/10.1061/(ASCE)GT.1943-5606.0001246)
- Whittle AJ, Davies RV (2006) Nicoll Highway collapse: evaluation of geotechnical factors affecting design of excavation support system. *International Conference on Deep Excavations*, Singapore. pp 28-30.
- Whittle AJ, Hashash YMA, Whitman RV (1993) Analysis of deep excavation in Boston. *Journal of Geotechnical and Geoenvironmental Engineering* 119: 69-90.
- Wong IH, Poh TY, Chuah HL (1997) Performance of excavations for depressed expressway in Singapore. *Journal of Geotechnical and Geoenvironmental Engineering* 123: 617-625. DOI: [10.1061/\(ASCE\)1090-0241\(1997\)123:7\(617\)](https://doi.org/10.1061/(ASCE)1090-0241(1997)123:7(617))
- Xu ZH, Wang JH, Wang WD (2008) Deformation behavior of diaphragm walls in deep excavations in Shanghai. *China Civil Engineering Journal* 41: 81-86. (In Chinese)
- Zheng G, Cheng XS, Diao Y (2011) Concept and design methodology of redundancy in braced excavation and case histories. *Geotechnical Engineering Journal of the SEAGS & AGSSEA* 42: 13-21.
- Zheng G, Li ZW (2012) Finite element analysis of response of the building with arbitrary angle adjacent to excavation. *Chinese Journal of Geotechnical Engineering* 34: 615-624. (In Chinese)